Applied Microbiology and Biotechnology (2022) 106:7139–7151
https://doi.org/10.1007/s00253-022-12196-3

APPLIED GENETICS AND MOLECULAR BIOTECHNOLOGY

Flavonoids from *Sedum aizoon* L. inhibit *Botrytis cinerea* by negatively affecting cell membrane lipid metabolism

Kaiyue Wang[1] · Xin Zhang[1] · Xingfeng Shao[1] · Yingying Wei[1] · Feng Xu[1] · Hongfei Wang[1]

Received: 23 February 2022 / Revised: 16 September 2022 / Accepted: 21 September 2022 / Published online: 6 October 2022

Abstract

Botrytis cinerea is a highly destructive and widespread phytopathogen in fruits. The widespread use of chemical antifungal agents on fruits has aided in disease control while their long-term use has resulted in the emergence of resistant fungal strains. Flavonoids have a specific antifungal effect. The inhibitory effect and underlying mechanism of flavonoids from *Sedum aizoon* L. (FSAL) on *B. cinerea* were determined in this study. The results showed that the minimum inhibitory concentration of FSAL against *B. cinerea* was 1.500 mg/mL. FSAL treatment caused leakage of macromolecules such as nucleic acids, led to accumulation of malondialdehyde and relative oxygen species, and disrupted the ultrastructure of *B. cinerea*. The transcriptome results indicated that compared with the control group, there were 782 and 1330 genes identified as being substantially upregulated and downregulated, respectively, in the FSAL-treated group. The identified genes and metabolites were mostly involved in redox processes and glycerolipid and amino acid metabolism pathways. FSAL offer a promising choice for food prevention and safety.

Key points

- *FSAL negatively affects the glycerolipid metabolism of B. cinerea*
- *FSAL minimum inhibitory concentration against B. cinerea was 1.500 mg/mL*
- *FSAL could be utilized as a new prevention strategy for gray mold in fruits*

Keywords Cell membrane · Mechanism · Flavonoids from *Sedum aizoon* L. · *Botrytis cinerea* · Glycerolipid metabolism

Introduction

Botrytis cinerea is a major pathogenic fungus that affects fruits such as grapes and strawberries (Li et al. 2020). It can infect more than 1400 species, including important crops such as strawberry, eggplant, tomato, and cucumber, and result in massive losses to fruit crops postharvest (Cui et al. 2021; Zambounis et al. 2020). Crop losses are particularly common during cold storage due to rots caused by fungi, which can result in significant economic losses (Wang et al. 2013). Currently, the use of synthetic chemical fungicides remains the most common method of preventing postharvest diseases. However, the excessive and frequent use of chemical fungicides has resulted in a number of negative impacts, such as environmental pollution, drug resistance, and several health issues (Nunes 2011). Consequently, novel plant-derived antifungal agents are favored for their safety and high efficacy.

Flavonoids are the most common natural plant-derived polyphenolic compounds, and they are abundant in grains, roots, seeds, leaves, fruits, and vegetables (Alsharairi 2021). Various protective effects of flavonoids have been reported, including antifungal and antimicrobial activities. For example, a previous study reported that the flavonoids in bee propolis can cause membrane destruction and nucleic acid leakage, which provides a basis for further research on the antifungal mechanisms of flavonoids (Manrique et al. 2008). *Sedum aizoon* L. is widely distributed in China and used as a traditional Chinese herbal medicine. It is rich in bioactive components, such as alkaloids, flavonoids, and

✉ Feng Xu
xufeng1@nbu.edu.cn

✉ Hongfei Wang
wanghongfei@nbu.edu.cn

[1] Zhejiang-Malaysia Joint Research Laboratory for Agricultural Product Processing and Nutrition, College of Food and Pharmaceutical Sciences, Ningbo University, Ningbo, China

polysaccharose (Xu et al. 2015). The flavonoids from *S. aizoon* L. (FSAL) in the leaves and stems have been characterized using high performance liquid chromatography (Waters Alliance E2695, Milford, MA, USA) (Luo et al. 2020) and identified as quercetin and kaempferol. Interestingly, our previous study (Wang et al. 2020) demonstrated the antibacterial activity of FSAL against *Shewanella putrefaciens*, which resulted in membrane damage and leakage of reducing sugars, DNA, and RNA. However, the antifungal mechanism of action of FSAL on *B. cinerea* is currently unknown. This study aimed to determine the inhibitory effects of FSAL on *B. cinerea* and the underlying mechanism.

Materials and methods

Preparation of FSAL

The FSAL was prepared as described by the study of Xu et al. (2018). *S. aizoon* L. samples were collected from Peixian County (Jiangsu, China), and the leaves and stems of *S. aizoon* L. were mainly used to prepare flavonoids. Then, they were dried and pulverized into a powder. Briefly, the sample was extracted with ethanol via rotary evaporation. The crude extract of flavonoids was purified using AB-8 macroporous resin (Beijing Solarbio Science & Technology Co., Ltd, Beijing, China) and then lyophilized after rotary evaporation to obtain a purified flavonoid sample, whose main components are quercetin and kaempferol. The purified sample was stored at – 80 ℃ until further use.

Fungal strain and culture conditions

B. cinerea (ACCC 36,028) was obtained from the Agricultural Culture Collection of China (Beijing, China), inoculated onto potato dextrose agar (PDA) (Hangzhou Microbial Reagent Co., Ltd, Hangzhou, China) plates, and cultured for 1 week at 25 ℃. The fungal spores were then scraped using a coating rod, rinsed with autoclaved pure water (Shuoguang Electronics Technology Co., Ltd, Shanghai, China), and collected and filtered through four layers of gauze (Shanghai Yongchuan Co., Ltd, Shanghai, China) to remove the hyphae. The spore count was adjusted to 1×10^6 spores/mL using a hematocytometer (Shanghai Yongchuan Co., Ltd, Shanghai, China).

Determination of the MIC

Different concentrations of FSAL (0.375, 0.750, 1.500, 3.000, and 6.000 mg/mL final concentration) were mixed with PDA medium and poured into Petri dishes to prepare a mixture of different basic FSAL concentrations. Additionally, control plates containing no FSAL were prepared. Each concentration was assigned six parallel groups. A 20 µL conidial suspension of *B. cinerea* (1×10^6 spores/mL) was added to the plates to create a uniform coating. The plates were cultured at 25 ℃ for 2 days, and the lowest flavonoid concentration without mycelium growth was considered the minimum inhibitory concentration (MIC) (Low et al. 2011). Based on standard operating procedures, MIC was defined as the lowest drug concentration that leads to a specific degree of visual fungal growth inhibition under specific incubation time and temperature conditions when performing a drug sensitivity test using an in vitro fungal dilution method or serial concentration gradient dilution method.

Measurement of cell membrane permeability

The content of extracellular nucleic acid in *B. cinerea* was determined via spectrophotometry (Xu et al. 2017). The spore suspension (1×10^6 spores/mL) was cultured at 25 ℃ for 0, 2, 4, 6, and 8 h. The supernatant was obtained by centrifuging the samples at 10,000 × g for 5 min at 4 ℃. Finally, the absorbance of the supernatant was measured at 260 nm using a UV spectrophotometer (Shanghai Meproda Instruments Co., Ltd, Shanghai, China) to determine intracellular nucleic acid leakage. The concentration of leaked proteins and total sugars were determined as previously described (Das et al. 2013). Electrical conductivity was determined as previously described (Cui et al. 2019) using a DDS-307 type conductivity meter (Mettler-Toledo Instruments Co., Ltd, Shanghai, China).

Detection of ROS

Reactive oxygen species (ROS) levels were measured using a previously reported method (Cui et al. 2019). The spores treated with FSAL (1 MIC) for 0, 2, and 4 h were collected. They were washed twice with phosphate-buffered saline (PBS; pH 7.4). The spore samples were stained using 10 µmol/L of 2′,7′-dichlorofluorescein diacetate (Nanjing Jiancheng Bioengineering Institute, Nanjing, China) dye solution in the dark. The samples were incubated on a floating plate in a water bath set to 37 ℃ for 30 min and then washed with PBS (pH 7.4). This step was repeated three times. A fluorescence microplate reader (Meigu molecular devices Co., Ltd, Shanghai, China) was used to determine the ROS level of *B. cinerea* and obtain the corresponding fluorescence intensity.

Ultrastructural observations using TEM

The ultrastructure of *B. cinerea* was observed using transmission electron microscopy (TEM) (Liu et al. 2017). *B.*

cinerea was inoculated into potato dextrose broth (PDB) medium and cultured at 25 ℃ and 120 rpm for 6 days, following which the culture was filtered through eight layers of gauze to obtain the mycelia. Then, the mycelia were treated with FSAL (1 MIC) for 4 h. The mycelia that were not treated with FSAL were used as the control. The FSAL-treated and control samples were filtered and washed three times with precooled PBS (pH 7.4), after which the mycelia were fixed overnight in 2.5% glutaraldehyde (Nanjing Bermuda Biotechnology Co., Ltd, Nanjing, China) (adjusted to pH 7.2 with 0.1 M PBS) at 4 ℃ and subsequently fixed with 1% osmic acid (Beijing Zhong mirror Instrument Technology Co., Ltd, Beijing, China) (adjusted to pH 7.2 with 0.2 M PBS) for 1–2 h. After washing the samples three times with 0.05 M PBS for 15 min each time, they were dehydrated with 30%, 50%, 70%, and 90% ethanol, 90% acetone and anhydrous acetone for 15 min each time. Finally, the samples were embedded in epoxy media (propylene oxide and epoxy resin [1:1]) and sliced into 70 nm sections using a diamond knife. The ultrathin slices were stained with uranyl acetate and lead citrate and observed and photographed using a transmission electron microscope (H-7650, Hitachi, Tokyo, Japan).

Determination of MDA content

Malondialdehyde (MDA) levels can be used to determine the degree of membrane lipid peroxidation (Ma et al. 2019). For determining the MDA content in *B. cinerea*, the spore suspensions were inoculated into PDB medium and cultured at 25 ℃ with shaking at 120 rpm for 48 h using a constant temperature oscillator, following which mycelia were collected. For each treatment, 3 g of mycelium was collected, with each treatment comprising three parallel groups. The samples were washed thrice with 0.1 M PBS (pH 7.0) and then suspended in the buffer. They were treated with FSAL (1 MIC), except the control samples, and collected at 0, 2, 4, 6, and 8 h after treatment. The MDA content of the samples was determined using a commercial kit (Nanjing Jiancheng Technology Co., Ltd, Nanjing, China) according to manufacturer's instructions.

RNA isolation, cDNA library construction, and sequencing

Spore suspensions (1×10^6 spores/mL) of *B. cinerea* were cultured in PDB medium for 7 days to obtain untreated mycelia. The FSAL-treated (1 MIC) and control mycelia were incubated at 25 ℃ for 4 h with shaking. The mycelia were collected and frozen in liquid nitrogen and stored at − 80 ℃ until RNA extraction.

Total RNA was isolated and purified using TRIzol (Invitrogen, Carlsbad, CA, USA). The NanoDrop ND-1000 spectrophotometer (NanoDrop, Wilmington, DE, USA) was used to quantify RNA and determine the purity of each sample. RNA integrity was validated via gel electrophoresis using Bioanalyzer 2100 (Agilent, CA, USA), and samples with an RNA integrity number of > 7.0 were selected for further analysis. These RNAs were reverse transcribed to cDNA and amplified using polymerase chain reaction (PCR) under the following conditions: initial denaturation at 95 ℃ for 3 min; 8 cycles of denaturation at 98 ℃ for 15 s, annealing at 60 ℃ for 15 s, and extension at 72 ℃ for 5 min. The average insert size of the cDNA library was 300 ± 50 base pairs (bp). Finally, the cDNA library was double-end sequenced using Illumina NovaSeq™ 6000 (LC-Bio Technology CO., Ltd., Hangzhou, China) in PE150 sequencing mode according to the standard protocol. Transcriptome analysis was performed using reference sequences from the NCBI database. (https://www.ncbi.nlm.nih.gov/genome/?term=Botrytis+cinerea).

Read mapping, annotation, and analysis

Sequencing using Illumina paired-end RNA sequencing (RNA-Seq) generated a total of millions of base pair (bp) length paired-end reads. Low-quality reads, including sequencing adapters, sequencing primers, and nucleotides with a q quality < 20, were discarded before assembly. Genes with ratio changes > twofold and $q < 0.05$ were defined as having significantly differential expression. We used a fold change (FC) of ≥ 2 or ≤ 0.5 (the absolute value of log2fc ≥ 1) as the change threshold, and $P < 0.05$ as the criteria for screening significantly differentially expressed genes (DEGs).

The unqualified sequences were removed to obtain valid data before proceeding with further analysis. The specific data preprocessing steps were as follows: removal of reads with the adapter; removal of reads that contain > 5% n (n represents the basic information that cannot be confirmed), and the removal of low-quality reads (a base number of $Q \leq 10$ indicates > 20% of the total reads). The initial sequencing quantity, effective sequencing quantity, GC content, Q20, and Q30 were counted and comprehensively evaluated.

Gene annotations of *B. cinerea* were obtained from the Genome Database (https://ftp.ncbi.nlm.nih.gov/genomes/all/GCF/000/143/535/GCF_000143535.2_ASM14353v4/GCF_000143535.2_ASM14353v4_genomic.fna.gz.). The genes were annotated using Gene Ontology (GO) enrichment (https://geneontology.org) and the Kyoto Encyclopedia of Genes and Genomes (KEGG) (https://www.kegg.jp/kegg) pathway analyses. These tools can also be used to predict related biochemical pathways.

The RNA-Seq data had been submitted to the Sequence Read Archive under accession number PRJNA880731 (http://www.ncbi.nlm.nih.gov/sra/PRJNA880731).

Analysis of DEGs

To compare the gene expression levels in various libraries, we evaluated the repeated relevance of six samples (three parallel FSAL treatments and control groups). FPKM (fragments per kilobase of exon model per million mapped fragments) was used to quantify the expression abundance of known genes across the six samples. The differential expression genes (DEGs) in samples treated with FSAL were screened using the combination criteria of log2 (FC) > 1 or log2 (FC) < − 1 and a *q* value of < 0.05 using the R package (Robinson et al. 2010).

Gene expression validation

To acquire the mycelia, *B. cinerea* spore suspensions (1×10^6 spores/mL) were grown in PDB medium for 7 days. The control and FSAL-treated (1 MIC) mycelia were incubated at 25 °C for 4 h while being shaken. Mycelia were then collected and immediately frozen in liquid nitrogen. Total RNA was extracted from each of the above sample using the Hipure fungal RNA extraction kit (Magen Biotechnology Co., Ltd, Guangzhou, China) according to the instructions of the kit, and the integrity of the RNA was examined using agarose gel electrophoresis, and the quality of the RNA was examined by a NanoDrop ND-2000 spectrophotometer (Thermo Scientific, Wilmington, USA). Primers were devised using the Illumina sequencing data with Premier 5 (Primer Company, Canada) (Table 1). A Vazyme HiScript II Q RT SuperMix for qPCR kit (VazymeBiotechCo., Ltd, Jiangsu, China) was used to prepare the cDNA from the isolated RNA. PCR was then performed using the ABI Prism 7500 Fast qPCR kit (Roche Switzerland Ltd., Basel, Switzerland) under the following conditions: 95 °C for 30 s for initial denaturation, 95 °C for 10 s, 60 °C for 30 s, a total of 40 cycles, then 95 °C for 10 s, 60 °C for 60 s, 95 °C for 15 s. The relative expression level of the target genes was determined using the $2^{-\Delta\Delta CT}$ method (Zhao et al. 2022). Primers for the internal reference gene were designed using the sequence for *BcActin* (accession number: XM001553318).

Statistical analysis

All experiments were performed in triplicate. Statistical analysis was performed using the SAS software package programme version 9.4 (SAS Institute, Cary, NC, USA). Comparisons among groups were analyzed using one-way analysis of variance. Duncan's multiple range test was used to determine significant differences based on a *P* level of < 0.05.

Results

MIC determination

The results of the MIC determination of FSAL against *B. cinerea* are presented in Table 2. FSAL was found to have a good inhibitory effect on *B. cinerea*. After 2 days of culture, when the FSAL concentration was ≥ 1.500 mg/mL, there was no evident colony growth, indicating that the MIC of FSAL for inhibiting *B. cinerea* was 1.500 mg/mL.

Table 1 Sequence of oligonucleotide primers used for the amplification of *Bcilv1*, *BCIN_07g07130*, *BCIN_08g03040*, *BCIN_10g02140*, *BCIN_11g02280*, *BCIN_14g05560*, and *BcActin*

Gene name	Function	Primer	Primer sequence (5′-3′)
Bcilv1	Isoleucine biosynthesis	*Bcilv1*-F	TTCTAACGGGTATTCTGTG
		Bcilv1-R	TCATCATCATAATCCTCCA
BCIN_07g07130	Electron transfer activity	*BCIN_07g07130*-F	TCGTTATTTGCGGCGTCTT
		BCIN_07g07130-R	TCTGTCCATGCTTCGGGTG
BCIN_08g03040	FAD binding	*BCIN_08g03040*-F	CTCGGTGTCATTGTCCCTG
		BCIN_08g03040-R	AATCTGATGCGTGGTCTCG
BCIN_10g02140	Integral component of the cell membrane	*BCIN_10g02140*-F	CATCCACAGAGTCCGTGAC
		BCIN_10g02140-R	CATACCAGTGCCAACTTCC
BCIN_11g02280	Cellular glucan metabolism	*BCIN_11g02280*-F	ACGCTACCGTTACCACTTT
		BCIN_11g02280-R	TGACTATCGTCCAGGAATT
BCIN_14g05560	Catalytic activity	*BCIN_14g05560*-F	TGTCCCGTATCGGTCCTCT
		BCIN_14g05560-R	CCAGCCGTGAAGCAAAGTG
BcActin	Actin formation	*BcActin*-F	CTCTATTCAAGCCGTCCTCTCC
		BcActin-R	TAATCAGTCAAATCACGACCAGC

Table 2 The MIC of flavonoids from *S. aizoon* L. on *B. cinerea*

Concentration of flavonoids from *S. aizoon* L. (mg/mL)						
Incubation time/d	6.00	3.00	1.50	0.75	0.375	0.00
2	-	-	-	+	+	+

"+" indicates significant colony growth; "-" indicates non-significant colony growth

Effect of FSAL treatment on B. *cinerea* cell membrane permeability

The results of the relative electrical conductivity and extracellular nucleic acid, total sugar, and protein contents of *B. cinerea* treated with FSAL for 0, 2, 4, 6, and 8 h are shown in Fig. 1. The nucleic acid content of the FSAL-treated groups showed an overall increasing trend (Fig. 1A). Significant leakage of intracellular nucleic acids was observed after 2 h of FSAL treatment ($P < 0.05$), which increased with increasing treatment time. The extracellular conductivity of *B. cinerea* increased initially with increasing treatment time but remained constant thereafter, with a similar trend observed between the treatment and control groups (Fig. 1B). However, the relative conductivity of the FSAL-treated group increased with increasing treatment time compared with the control group ($P < 0.05$), indicating that FSAL treatment increased the membrane permeability of *B. cinerea* and partially disrupted ionic homeostasis. The total sugar content in the FSAL-treated group increased with the treatment time and was markedly higher than that in the control group. After 2 h of FSAL exposure, the total sugar content in the treatment group was 102.86 μg/mL, which was markedly higher than that in the control group ($P < 0.05$), and the total sugar content reached 178.33 μg/mL. An increase in the total sugar content indicated extracellular sugar leakage, implying a change in cell membrane permeability (Fig. 1C). With increasing treatment time, the protein content in the FSAL-treated group increased and was higher than that in the control group (Fig. 1D). After 8 h of FSAL exposure, the protein content in the treatment group was 90.14 μg/mL, which was markedly higher than that in the control group ($P < 0.05$). Taken together, these results indicated that FSAL treatment damaged the cell membrane of *B. cinerea*.

Effect of FSAL on the accumulation of ROS in B. *cinerea*

The results of ROS levels in *B. cinerea* treated with FSAL for 0, 2, 4, 6, and 8 h are shown in Fig. 2. The fluorescence intensity in the FSAL-treated group increased and then decreased. However, in the control group, it only decreased slightly. The fluorescence intensity represented the ROS level. The FSAL treatment significantly increased ROS accumulation, with the treatment group having higher ROS levels than the control group. These results indicated that FSAL induced oxidative stress and resulted in peroxidative damage in *B. cinerea*.

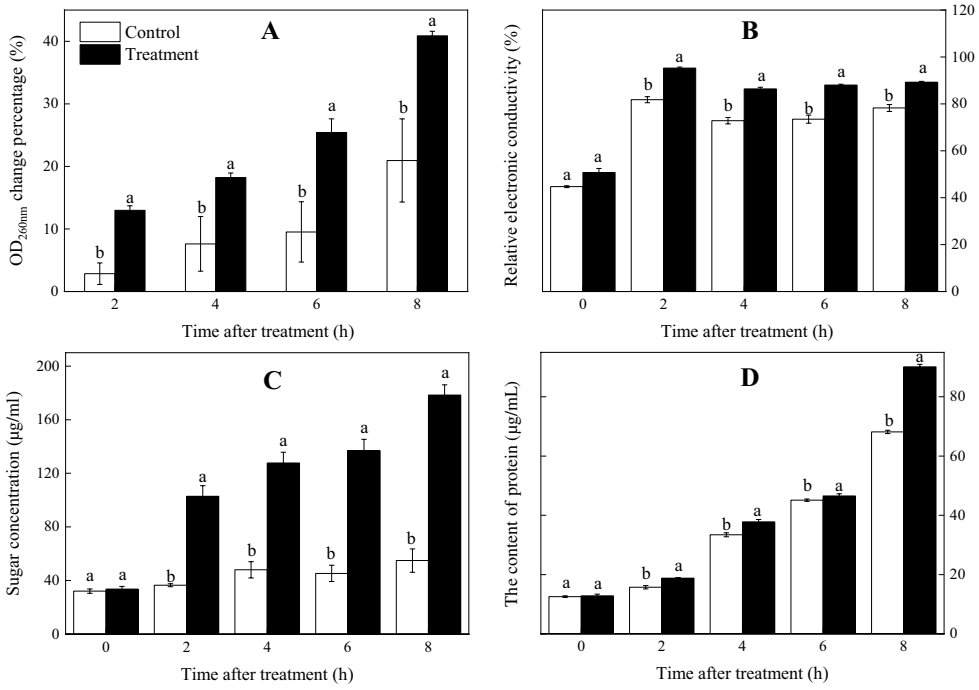

Fig. 1 The effect of membrane permeability of *B. cinerea* cells by FSAL (1.0 MIC), the control group was treated with pure water. The nucleic acids content (**A**), the relative conductivity (**B**), the total sugar content (**C**) and the protein content (**D**) of the fungal culture. Different letters (a, b) indicate significant differences at $p < 0.05$ level. The error bar shows the standard deviation

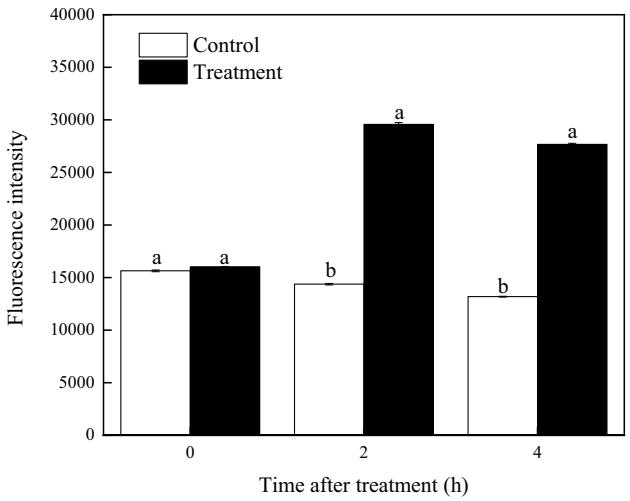

Fig. 2 Effects of FSAL (1.0 MIC) treatment on intracellular ROS content of *B. cinerea* cells, and the control group was treated with pure water. Different letters (a, b) indicate significant differences at $p < 0.05$ level. The error bar shows the standard deviation

Effect of FSAL treatment on the ultrastructure of *B. cinerea*

The ultrastructure of the *B. cinerea* mycelia treated with FSAL was observed via TEM (Fig. 3). The mycelium of the control (Fig. 3A) clearly showed the cell wall, cytoplasm, cell membrane, and normal organelle structures. Conversely, in *B. cinerea* treated with FSAL, the organelles (such as the mitochondria) were degraded, the integrity of the cell membrane was destroyed, and vesicles and cavities appeared inside the cells (Fig. 3B). These results showed that FSAL disrupted the cell membrane of *B. cinerea*.

Effect of FSAL treatment on MDA content of *B. cinerea*

The results of MDA content in *B. cinerea* treated with FSAL for 0, 2, 4, 6, and 8 h are shown in Fig. 4. The MDA content in the FSAL-treated group was significantly higher than that in the control group, especially as the value of MDA was 8.428 nmol/mg at 4 h ($P < 0.05$). The data indicated that FSAL increased the rate and intensity of lipid peroxidation and worsened the degree of peroxidative damage in *B. cinerea*.

Illumina sequence data

Six isolated libraries (biological replicates) were constructed for RNA-Seq, representing the transcriptomes of each of the three control samples (Control_1 – Control_3) and the three FSAL-treated samples (Treat_1 – Treat_3; Supplemental Table S1). A total of 29.24 gigabyte (GB) of valid data were obtained. For ≥ 97% of the reads, the average quality value per sample was ≥ 30. The six samples had a GC content of 46% ± 1%. The reads for each library were mapped to the genome of *B. cinerea* at a rate of > 93% for the FSAL-treated library and > 94% for the control library. The results showed that the library structure and reads generated from RNA-Seq were of good quality.

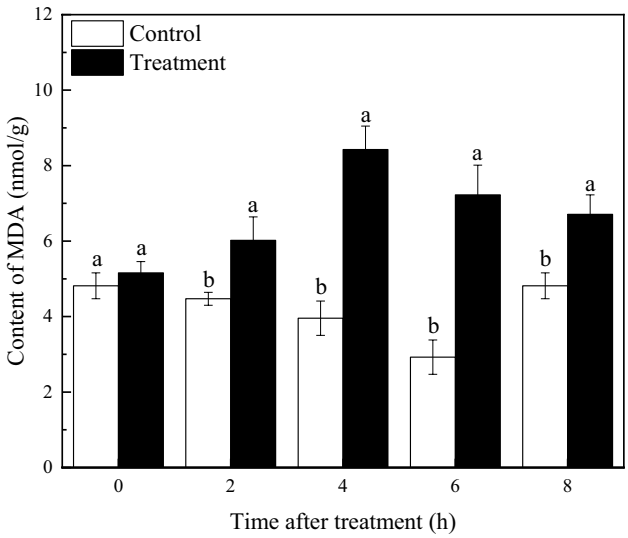

Fig. 4 Effects of FSAL (1.0 MIC) on malondialdehyde contents of *B. cinerea* cells, and the control group was treated with pure water. Different letters (a, b) indicate significant differences at $p < 0.05$ level. The error bar shows the standard deviation

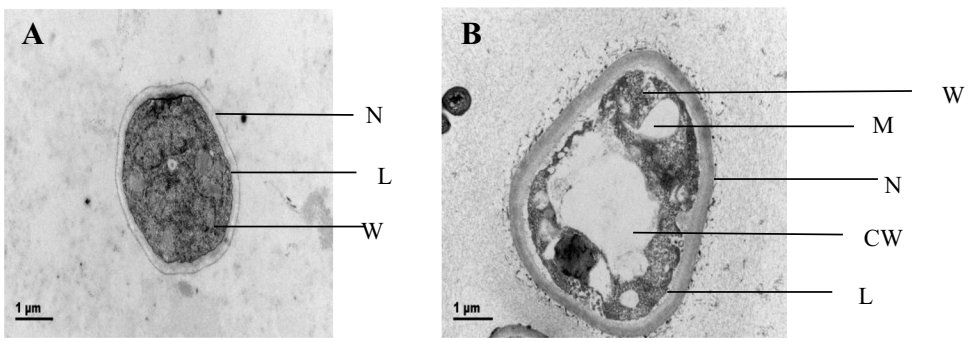

Fig. 3 Effect of FSAL on the ultrastructure of *B. cinerea*. **A** TEM image of *B. cinerea* without the treatment of FSAL (control). **B** TEM image of *B. cinerea* after the treatment of FSAL (1.0 MIC) for 4 h. L, cell membrane; M, vesicle; N, cell wall; W, cytoplasm; CW, the cavity of the cytoplasm

Gene expression analysis

HTSeq statistical analysis was used to analyze the FPKM interval (0–1, 1–3, 3–15, 15–60, and > 60) gene expression outcomes (Supplemental Fig. S1). As shown in Table 3, the FSAL treatment and control groups had different gene expression statistics at each FPKM interval. Owing to differences in the number of genes and the distribution of gene expression values across the samples, it was possible to divide sample expression values into different intervals and calculate the number of genes expressed across the samples at the different expression intervals.

Defining DEGs

After the treatment with 1 MIC FSAL, 2112 DEGs were identified between the FSAL and control groups, including 782 and 1330 upregulated and downregulated genes, respectively (Fig. 5). Supplemental Table S2 and Table 4 show the DEGs between the FSAL-treated and control groups. FSAL treatment downregulated the genes related to glycerolipid metabolism (*BCIN_10g04190*), fungal-type cell wall (*Bcgas2*), and proteolysis (*BCIN_05g06240*). In contrast, FSAL upregulated the genes associated with apoptotic process (*Bclot6*), fatty acid degradation (*BCIN_01g11030*), xenobiotic transmembrane transporting ATPase activity (*Bmr3*), polygalacturonase activity (*BcPG3*), and DNA replication (*Bcap4*).

Gene function classification using GO enrichment analysis

To further understand the functional categories of the DEGs after FSAL treatment. DEG enrichment analysis was performed (Fig. 6 and Supplemental Table S3). The DEGs were classified into three GO categories: cellular component, biological process, and molecular function, which were composed of 25, 15, and 10 subcategories, respectively. In the biological processes category, FSAL promoted acid phosphatase activity via upregulation of *Bcltp1* and *BCIN_07g04290*. Genes associated with components of the plasma membrane (e.g., *Bchex2*, *Bchxt19*, *Bcpho89*, *Bcctr1*, *Bcdip5*) were mainly downregulated in the FSAL-treated groups. In the cellular components category, FSAL caused upregulation of genes related to oxidation–reduction process (e.g., *Bcgod1*, *Bctrr1*, and *Bcaif1*). In contrast, FSAL downregulated genes associated with integral component of plasma membrane (e.g., *Bchnm1*, *Bcgit1*, and *Bcstl1*) and genes associated with glucose transmembrane transporter activity and glucose import (e.g., *Bchxt15*, *Bchex2*, and *Bchxt19*). In molecular function category, FSAL treatment upregulated the genes associated with metabolic process such as *Bcpcs60*, *Bcfmp41*, and *Bclsc2*, and downregulated genes such as *Bcpks20*, *Bmr5*, and *Bcayr1*.

KEGG pathway analysis

KEGG enrichment analysis of DEG functions was performed using bioinformatics databases (Fig. 7, Supplemental Table S4). The results revealed that the significantly DEGs were enriched in the following KEGG pathways: glycerolipid metabolism, degradation of amino acids (such as valine, leucine and isoleucine), starch and sucrose metabolism, butanoate metabolism, ABC transporter, and sulfur metabolism. The gene encoding triacylglycerol lipase (*Bctgl2*), and the gene encoding diacylglycerol acyltransferase of phospholipids (*Bclro1*), were upregulated. The upregulation of genes associated with lysophospholipases (e.g., *Bclpl1* and *Bcnte1*) indicated that FSAL treatment enhanced phospholipase activity and thus accelerated membrane phospholipid degradation. In addition, genes related to fatty acid catabolic process and triglyceride biosynthetic process (*Bcpah1*) were downregulated, as well as genes related to lysophosphatidic acid acyltransferase (*Bcale1*) and fatty acid elongation (*Bcphs1*). Besides, FSAL resulted in upregulation of genes associated with the degradation of valine, leucine and isoleucine (e.g., *Bcpot1*, *Bcpio2*, *Bcuga1*, and *Bcehd3*). These results demonstrated that FSAL affected glycerolipid and amino acid metabolism in *B. cinerea*.

Table 3 Statistics of the number of expressed genes in different FPKM interval samples

Sample	0 – 0.1 FI	0.1 – 0.3 FI	0.3 – 3.57 FI	3.57 – 15 FI	15 – 60 FI	>60 FI
Control_1	1049 (8.97%)	525 (4.49%)	2441 (20.87%)	2715 (23.21%)	3294 (28.16%)	1674 (14.31%)
Control_2	1043 (8.92%)	527 (4.51%)	2416 (20.65%)	2721 (23.26%)	3293 (28.15%)	1698 (14.52%)
Control_3	938 (8.02%)	496 (4.24%)	2678 (22.89%)	2996 (25.61%)	3026 (25.87%)	1564 (13.37%)
Treat_1	841 (7.19%)	500 (4.27%)	2870 (24.53%)	2803 (23.96%)	3037 (25.96%)	1647 (14.08%)
Treat_2	1156 (9.88%)	704 (6.02%)	2646 (22.62%)	2584 (22.09%)	2881 (24.63%)	1727 (14.76%)
Treat_3	1142 (9.76%)	631 (5.39%)	2618 (22.38%)	2706 (23.13%)	2973 (25.41%)	1628 (13.92%)

"FI" is the abbreviation of FPKM interval, which indicates the level of expression value of a sample

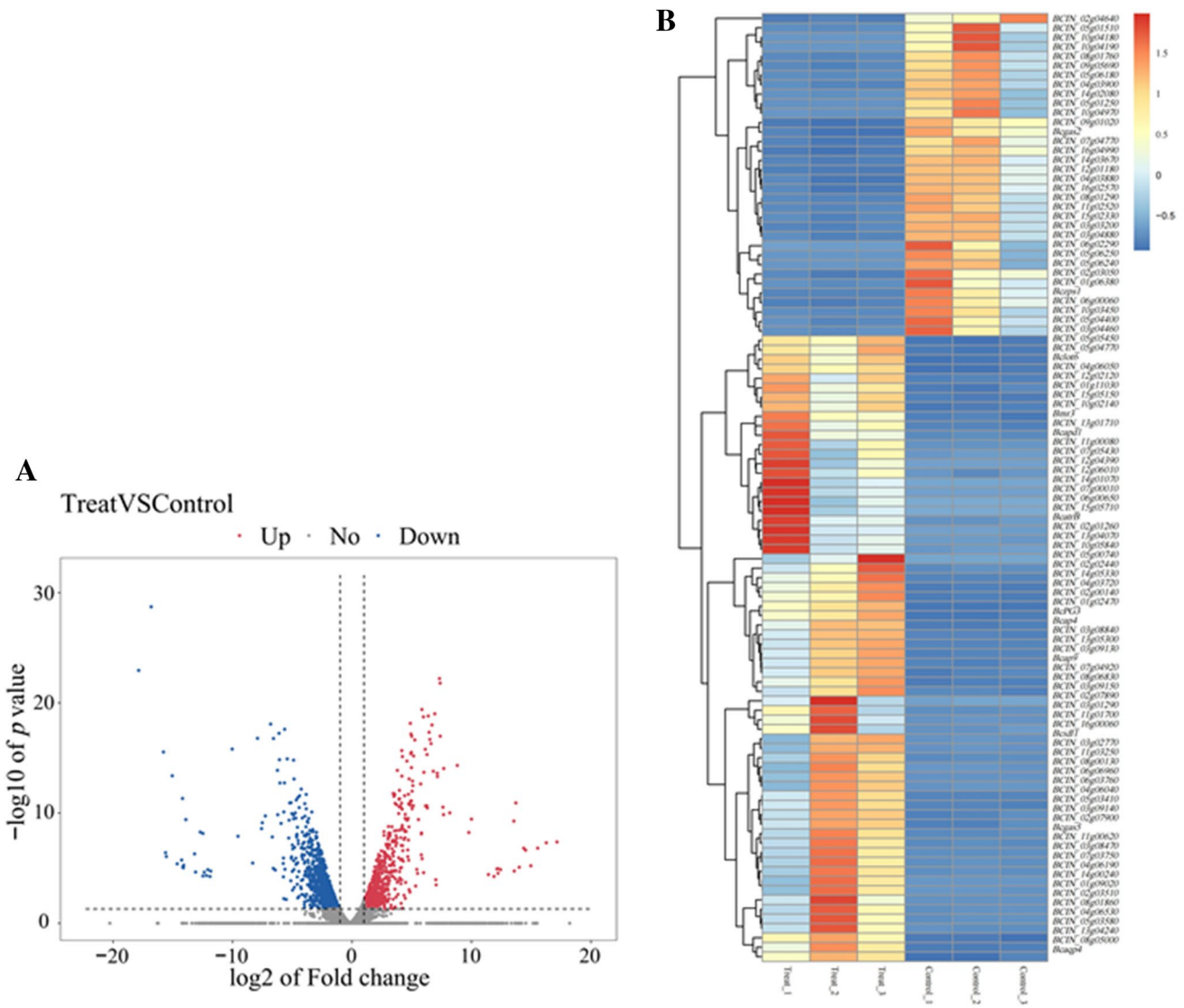

Fig. 5 Analysis of differentially expressed genes in *B. cinerea* (FSAL-treated and control groups). **A** Each dot represents a gene, and the up-regulated genes (red rots) and down-regulated genes (blue rots) are significantly different for each group shown on the volcano plot. **B** All DEGs between the FSAL-treated (Treat_1 – Treat_3) and control groups (Control_1 – Control_3) are shown on the heatmap. Low-expressed genes are represented by the dark blue cluster, while highly expressed genes are represented by the red cluster

QRT-PCR analysis of DEGs obtained from RNA-Seq

Six genes were selected for qRT-PCR to validate the transcriptome analysis results. These genes are involved in isoleucine biosynthesis, electron transfer activity, flavin adenine dinucleotide (an integral component of the membrane) binding, cellular glucan metabolism, and catalytic activity, and they were randomly selected for primarily verifying the accuracy of the transcriptome analysis results. As shown in Fig. 8, after the FSAL treatment, the expression levels of *Bcilv1*, *BCIN_08g03040*, and *BCIN_10g02140* were upregulated, while those of *BCIN_07g07130*, *BCIN_11g02280*, and *BCIN_14g05560* were downregulated. This finding indicates the agreement between these results and the RNA-Seq data, further indicating the reliability of the transcriptome data.

Discussion

Many relevant plant-derived antifungal agents have been reported. The essential oil of *Eucalyptus* has been shown to inhibit the mycelia and conidia of *B. cinerea* (Pedrotti et al. 2019). Fennel and peppermint essential oils can inhibit the growth of *B. cinerea* in plum fruits (Aminifard and Mohammadi 2013). In the present study, FSAL treatment disrupted cell membrane and ultrastructure of *B. cinerea* (Fig. 3).

The accumulation of ROS caused membrane lipid peroxidative damage in the organism (Yin et al. 2011) and changed the fatty acid content in the cell membrane, resulting in cell membrane damage. Tea tree essential oil may cause mitochondrial dysfunction and oxidative stress in *B. cinerea* (Li

Table 4 Major DEGs and their functions between the FSAL-treated and the control groups

Gene name	Functions	Up- or down-regulated
BCIN_10g04190	Glycerolipid metabolism	Down
Bcgas2	Fungal-type cell wall	Down
BCIN_05g06240	Proteolysis	Down
Bclot6	Apoptotic process	Up
BCIN_01g11030	Fatty acid degradation	Up
Bmr3	Xenobiotic transmembrane transporting ATPase activity	Up
BcPG3	Polygalacturonase activity	Up
Bcap4	DNA replication	Up
Bcltp1	Acid phosphatase activity	Up
Bchex2	Components of the plasma membrane	Down
Bcgod1	Oxidation–reduction process	Up
Bchnm1	Integral component of plasma membrane	Down
Bchxt15	Glucose import	Down
Bcpcs60	Metabolic process	Up
Bcpks20	Metabolic process	Down
Bctgl2	Triacylglycerol lipase	Up
Bclro1	Diacylglycerol acyltransferase	Up
Bclpl1	Lysophospholipases	Up
Bcpah1	Fatty acid catabolic process	Down
Bcale1	Lysophosphatidic acid acyltransferase	Down
Bcpot1	Degradation of valine, leucine and isoleucine	Up
Bcphs1	Fatty acid elongation	Down

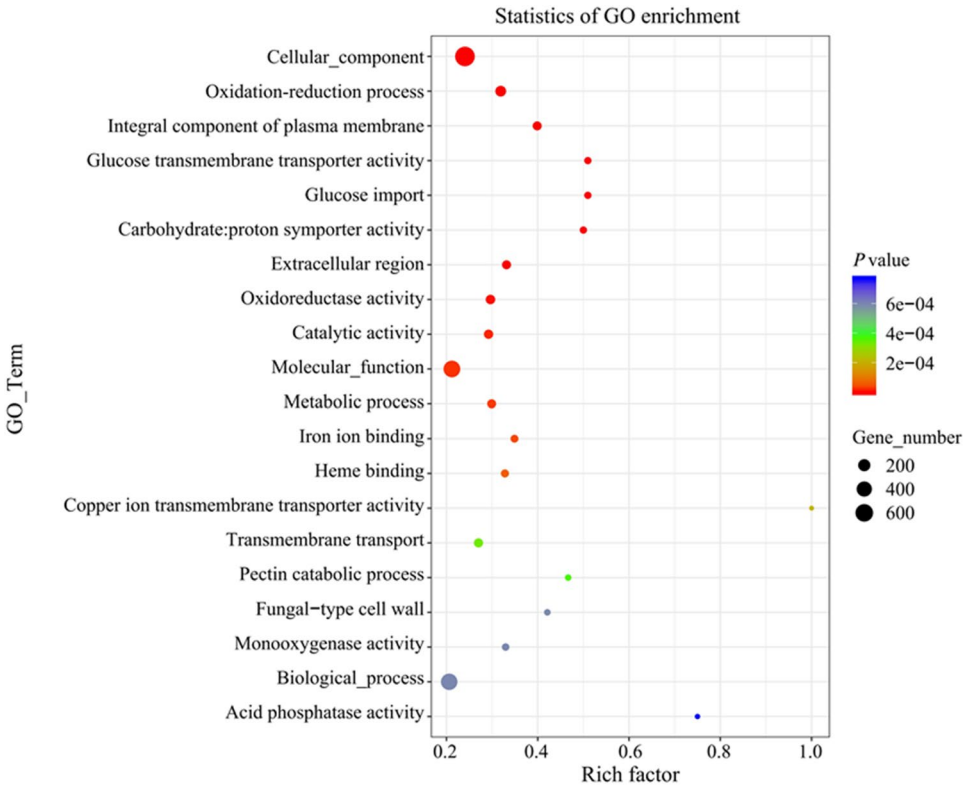

Fig. 6 GO enrichment analysis was performed on DEGs between the treatment of FSAL group and control group. The horizontal axis indicates the degree of enrichment, the vertical axis indicates the enriched GO term; the size of the dots indicates the number of differential genes enriched to a GO term; the color of the dots indicates different *p* values; the rich factor indicates the number of differential genes belonging to a GO term and the total number of genes belonging to the GO

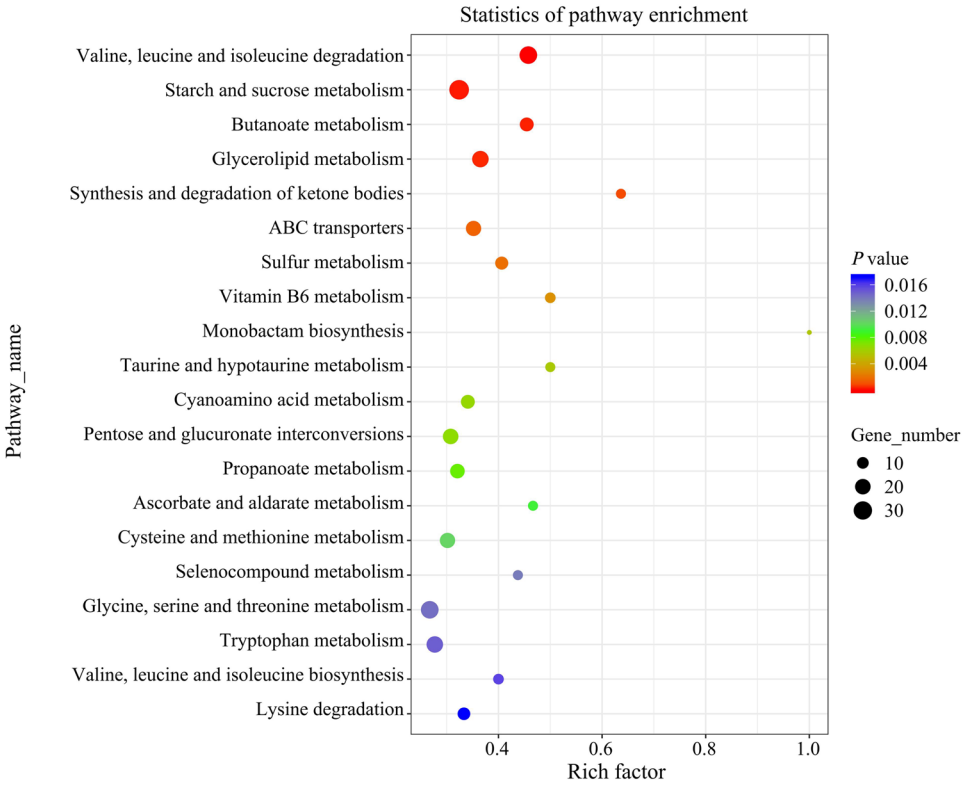

Fig. 7 KEGG enrichment analysis of DEGs between FSAL-treated and control groups was performed. The horizontal axis indicates the degree of enrichment and the vertical axis indicates the enriched KEGG pathway; the size of the dots indicates the number of differential genes enriched to a certain KEGG pathway; the color of the dots indicates different *p* values; the rich factor indicates the number of differential genes belonging to a certain KEGG pathway and the total number of genes belonging to this KEGG pathway

et al. 2020). Baicalein and wogonin have been shown to accumulate ROS and disrupt mitochondrial metabolism in *Aspergillus fumigatus*, leading to apoptosis (Da et al. 2019). In our work, FSAL treatment can induce the accumulation of ROS and MDA, cause degradation of organelles such as mitochondria, and also bring about an increase in conductivity and leakage of cell contents in *B. cinerea*. This is consistent with the findings of previous report that FSAL treatment resulted in the leakage of cellular contents of *Penicillium italicum* via cell membrane disruption (Luo et al. 2020).

The cell membranes of fungi are rich in lipids belonging to the glycerophospholipid, sphingolipid, and sterol classes (Sant et al. 2016). These lipids create a significant barrier structure between the cytoplasm and extracellular medium and play an important role in regulating cellular metabolism and energy transduction (Sanchez et al. 2010). Glycerolipid plays a major role in the membrane structure, and the ratio of unsaturated to saturated fatty acids (Athenstaedt 2021) in glycerolipid metabolism show a significant effect on cell membranes (Wang et al. 2022). In the present study, FSAL downregulated the *Bcale1* gene in *B. cinerea*. In *Saccharomyces cerevisiae*, *SLC1* has been identified as the gene encoding a lysophosphatidic acid acyltransferase, which catalyzes the synthesis of phosphatidic acid (Benghezal et al. 2007), while *LPT1* has also been shown to be involved in the acylation of lysophospholipids in *S. cerevisiae* (Tamaki et al. 2007). The *Bcale1* gene in this study also encoded a lysophosphatidic acid acyltransferase and may have effects on glycerolipid metabolism and even the cell membrane in *B. cinerea*. Meanwhile, the genes involved in the process of fatty acid catabolism, the biosynthesis of triglycerides (*Bcpah1*, *Bcpex7*) and fatty acid elongation (*Bcphs1*) were downregulated, indicating that FSAL interferes with the lipid metabolism of *B. cinerea*. A similar study has been reported that chitosan has an inhibitory effect on the lipid metabolism of *Phytophthora infestans* (Huang et al. 2021).

The amino acid composition is closely associated with membrane structure, as membrane proteins are the main bearers of biological membrane function (Zuo et al. 2005). Proteins embedded in the interior of the lipid bilayer of the membrane are composed of a number of nonpolar amino acids that bind to the hydrophobic tails of lipid molecules (Yildirim et al. 2007). In *B. cinerea*, the *Bcpio3* has been shown to be calcium neuron dependent and may be a calcium regulatory protein (Gioti et al. 2006). In the present study, FSAL upregulated genes related to the degradation of valine, leucine and isoleucine (e.g., *Bcpot1*, *Bcpio2*, *Bcuga1*, and *Bcehd3*), which suggested that FSAL affected the amino acid metabolism and even protein metabolism of *B. cinerea*. Glutamate is known to have a protective effect on cell membranes, which is related to its ability to interact with the lipid bilayer of the cell membrane (Martos et al. 2007). Differential genes related to glutamate metabolism (e.g., *Bcgdh2*, *Bcuga2*, *Bcgln1*, and *Bcmsc7*), and encoding L-glutamate transmembrane transporter activity (*Bcdip5*) were notably downregulated under FSAL treatment, and

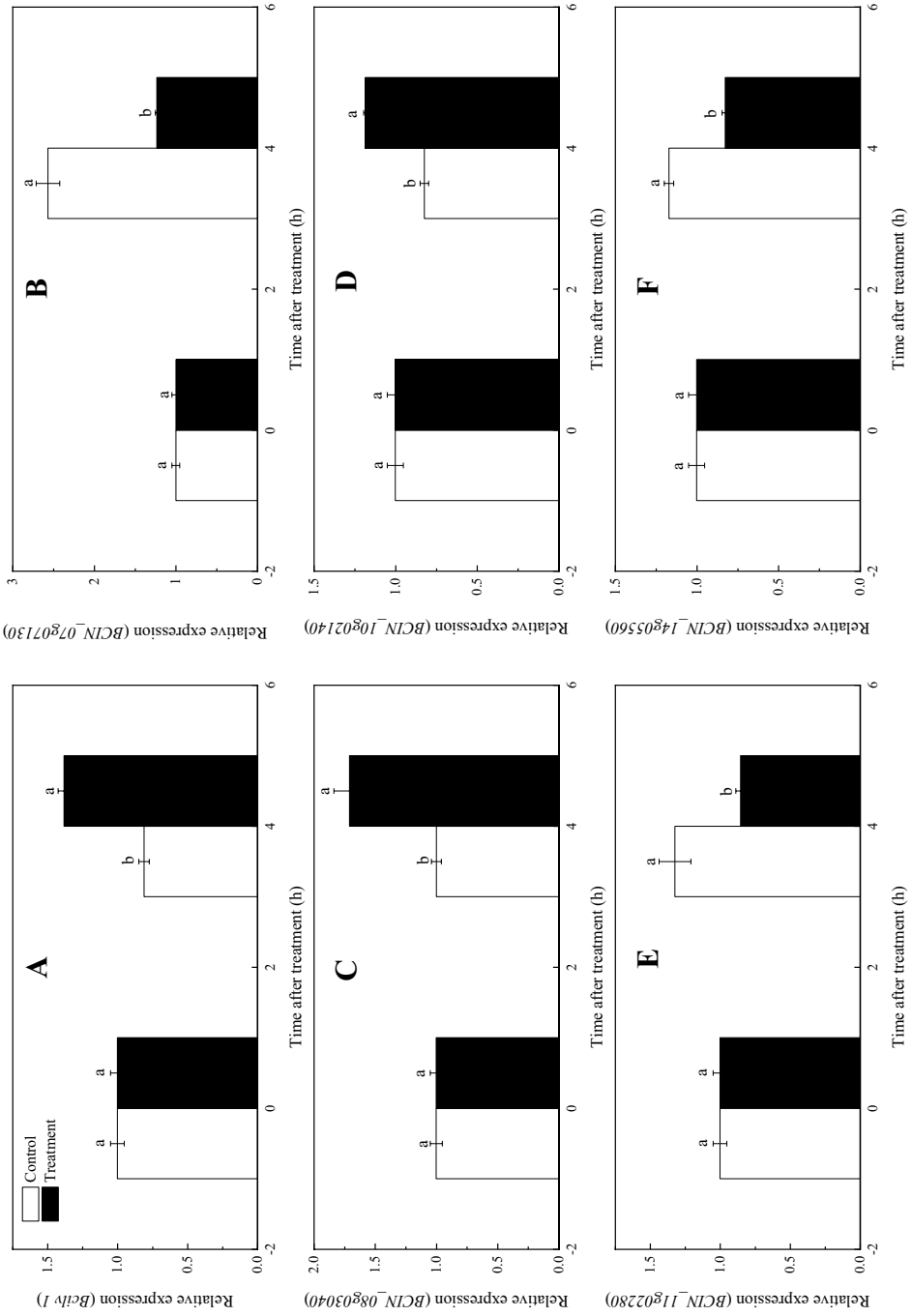

Fig. 8 Expression of levels of *Bcilv1* (**A**), *BCIN_07g07130* (**B**), *BCIN_08g03040* (**C**), *BCIN_10g02140* (**D**), *BCIN_11g02280* (**E**), and *BCIN_14g05560* (**F**). Different letters indicate significant differences at $p < 0.05$ level. The error bar shows the standard deviation

attenuated the protective capacity of the cell membrane. Similarly, amino acid metabolism induced by a natural trisaccharide ester from the cultures of *Pezicula neosporulosa* may have a strong influence on the inhibition of *Geotrichum citri-aurantii* (Xu et al. 2022).

In conclusion, this study demonstrated that FSAL treatment induced the accumulation of ROS and MDA and disrupted the cell membrane structure of *B. cinerea*. Transcriptomic analysis revealed that FSAL mainly reacted via the regulation of the pathways of glycerolipid and amino acid metabolism and damage of cell membrane of *B. cinerea*. Our study findings may facilitate the development of antifungal agents with a natural plant origin and provide a basis for fruit preservation applications.

Supplementary Information The online version contains supplementary material available at https://doi.org/10.1007/s00253-022-12196-3.

Author contribution KYW: investigation, formal analysis and writing-original draft. XZ: methodology. XFS: writing—review and editing. YYW: data curation. FX: resources, validation and visualization. HFW: conceptualization, supervision, and project administration.

Funding This research was supported through funding from the Public Welfare Applied Research Project of Ningbo City (2022S138 and 2022S154) and Student Research and Innovation Programme of Ningbo University (2021SRIP3607).

Data availability The data sets generated and/or analyzed during this study can be reasonably requested from the corresponding authors.

Declarations

Ethics approval This article does not contain any studies with human participants or animals performed by any of the authors.

Conflict of interest The authors declare no competing interests.

References

Alsharairi NA (2021) *Scutellaria baicalensis* and their natural flavone compounds as potential medicinal drugs for the treatment of nicotine-induced non-small-cell lung cancer and asthma. Int J Environ Res Public Health 18:5243. https://doi.org/10.3390/ijerph18105243

Aminifard MH, Mohammadi S (2013) Essential oils to control *Botrytis cinerea in vitro* and *in vivo* on plum fruits. J Sci Food Agric 93(2):348–353. https://doi.org/10.1002/jsfa.5765

Athenstaedt K (2021) Phosphatidic acid biosynthesis in the model organism yeast *Saccharomyces cerevisiae* - a survey. BBA-Mol Cell Biol L 1866(6):158907. https://doi.org/10.1016/j.bbalip.2021.158907

Benghezal M, Roubaty C, Veepuri V, Knudsen J, Conzelmann A (2007) *SLC1* and *SLC4* encode partially redundant acyl-coenzyme A 1-acylglycerol-3-phosphate *O*-acyltransferases of budding yeast. J Biol Chem 282(42):30845–30855. https://doi.org/10.1074/jbc.M702719200

Cui H, Zhang C, Li C, Lin L (2019) Antibacterial mechanism of oregano essential oil. Ind Crops Prod 139:111498. https://doi.org/10.1016/j.indcrop.2019.111498

Cui X, Ma D, Liu X, Zhang Z, Li B, Xu Y, Chen T, Tian S (2021) Magnolol inhibits gray mold on postharvest fruit by inducing autophagic activity of *Botrytis cinerea*. Postharvest Biol Tec 180:111596. https://doi.org/10.1016/j.postharvbio.2021.111596

Da X, Nishiyama Y, Tie D, Hein KZ, Yamamoto O, Morita E (2019) Antifungal activity and mechanism of action of Ou-gon (*Scutellaria* root extract) components against pathogenic fungi. Sci Rep 9:1683. https://doi.org/10.1038/s41598-019-38916-w

Das MR, Sarma RK, Borah S, Kumari R, Saikia R, Deshmukh AB, Shelke MV, Sengupta P, Szunerits S, Boukherroub R (2013) The synthesis of citrate-modified silver nanoparticles in an aqueous suspension of graphene oxide nanosheets and their antibacterial activity. Colloids Surf B 105:128–136. https://doi.org/10.1016/j.colsurfb.2012.12.033

Gioti A, Simon A, Pêcheur PL, Giraud C, Pradier JM, Viaud M, Levis C (2006) Expression profiling of *Botrytis cinerea* genes identifies three patterns of up-regulation *in planta* and an FKBP12 protein affecting pathogenicity. J Mol Biol 358(2):372–386. https://doi.org/10.1016/j.jmb.2006.01.076

Huang X, You Z, Luo Y, Yang C, Ren J, Liu Y, Wei G, Dong P, Ren M (2021) Antifungal activity of chitosan against *Phytophthora infestans*, the pathogen of potato late blight. Int J Biol Macromol 166:1365–1376. https://doi.org/10.1016/j.ijbiomac.2020.11.016

Li Z, Shao X, Wei Y, Dai K, Xu J, Xu F, Wang H (2020) Transcriptome analysis of *Botrytis cinerea* in response to tea tree oil and its two characteristic components. Appl Microbiol Biotechnol 104(5):2163–2178. https://doi.org/10.1007/s00253-020-10382-9

Liu G, Ren G, Zhao L, Cheng L, Wang C, Sun B (2017) Antibacterial activity and mechanism of bifidocin A against *Listeria monocytogenes*. Food Control 73:854–861. https://doi.org/10.1016/j.foodcont.2016.09.036

Low WL, Martin C, Hill DJ, Kenward MA (2011) Antimicrobial efficacy of silver ions in combination with tea tree oil against *Pseudomonas aeruginosa*, *Staphylococcus aureus* and *Candida albicans*. Int J Antimicrob Agents 37:162–165. https://doi.org/10.1016/j.ijantimicag.2010.10.015

Luo J, Xu F, Zhang X, Shao X, Wei Y, Wang H (2020) Transcriptome analysis of *Penicillium italicum* in response to the flavonoids from *Sedum aizoon* L. World J Microbiol Biotechnol 36:62. https://doi.org/10.1007/s11274-020-02836-z

Ma D, Ji D, Zhang Z, Li B, Qin G, Xu Y, Chen T, Tian S (2019) Efficacy of rapamycin in modulating autophagic activity of *Botrytis cinerea* for controlling gray mold. Postharvest Biol Tec 150:158–165. https://doi.org/10.1016/j.postharvbio.2019.01.005

Manrique JA, Santana CW (2008) Flavonoids, antibacterial and antioxidant activities of propolis of stingless bees, Melipona quadrifasciata, Melipona compressipes, Tetragonisca angustula, and Nannotrigona sp. from Brazil and Venezuela. Zootecnia Tropical 26(2):157–166

Martos GI, Minahk CJ, Font G, de Valdez MR (2007) Effects of protective agents on membrane fluidity of freeze-dried *Lactobacillus delbrueckii* ssp. *bulgaricus*. Lett Appl Microbiol 45:282–288. https://doi.org/10.1111/j.1472-765X.2007.02188.x

Nunes CA (2011) Biological control of postharvest diseases of fruit. Eur J Plant Pathol 133:181–196. https://doi.org/10.1007/s10658-011-9919-7

Pedrotti C, Marcon AR, Longaray Delamare AP, Echeverrigaray S, da Silva Ribeiro RT, Schwambach J (2019) Alternative control of grape rots by essential oils of two *Eucalyptus* species. J Sci Food Agric 99:6552–6561. https://doi.org/10.1002/jsfa.9936

Robinson MD, McCarthy DJ, Smyth GK (2010) edgeR: a Bioconductor package for differential expression analysis of digital gene

expression data. Bioinformatics 26:139–140. https://doi.org/10.1093/bioinformatics/btp616
Sanchez E, Garcia S, Heredia N (2010) Extracts of edible and medicinal plants damage membranes of *Vibrio cholerae*. Appl Environ Microbiol 76:6888–6894. https://doi.org/10.1128/AEM.03052-09
Sant DG, Tupe SG, Ramana CV, Deshpande MV (2016) Fungal cell membrane-promising drug target for antifungal therapy. J Appl Microbiol 121:1498–1510. https://doi.org/10.1111/jam.13301
Tamaki H, Shimada A, Ito Y, Ohya M, Takase J, Miyashita M, Miyagawa H, Nozaki H, Nakayama R, Kumagai H (2007) *LPT1* encodes a membrane-bound *O*-acyltransferase involved in the acylation of lysophospholipids in the yeast *Saccharomyces cerevisiae*. J Biol Chem 282(47):34288–34298. https://doi.org/10.1074/jbc.M704509200
Wang J, Chi Z, Zhao K, Wang H, Zhang X, Xu F, Shao X, Wei Y (2020) A transcriptome analysis of the antibacterial mechanism of flavonoids from Sedum aizoon L. against Shewanella putrefaciens. World J Microbiol Biotechnol 36:94. https://doi.org/10.1007/s11274-020-02871-w
Wang J, Xia X, Wang H, Li P, Wang K (2013) Inhibitory effect of lactoferrin against gray mould on tomato plants caused by *Botrytis cinerea* and possible mechanisms of action. Int J Food Microbiol 161:151–157. https://doi.org/10.1016/j.ijfoodmicro.2012.11.025
Wang Y, Zhai J, Qi Z, Liu W, Cui J, Zhang X, Bai S, Li L, Shui G, Cui S (2022) The specific glycerolipid composition is responsible for maintaining the membrane stability of *Physcomitrella patens* under dehydration stress. J Plant Physiol 268:153590. https://doi.org/10.1016/j.jplph.2021.153590
Xu F, Wang C, Wang H, Xiong Q, Wei Y, Shao X (2018) Antimicrobial action of flavonoids from *Sedum aizoon* L. against lactic acid bacteria *in vitro* and in refrigerated fresh pork meat. J Funct Foods 40:744–750. https://doi.org/10.1016/j.jff.2017.09.030
Xu J, Shao X, Li Y, Wei Y, Xu F, Wang H (2017) Metabolomic analysis and mode of action of metabolites of tea tree oil involved in the suppression of *Botrytis cinerea*. Front Microbiol 8:1017. https://doi.org/10.3389/fmicb.2017.01017
Xu L, Feng L, Sun J, Mao L, Li X, Jiang Y, Duan X, Li T (2022) Antifungal activities of a natural trisaccharide ester against sour rot in mandarin fruit. Postharvest Biol Tec 191:111981. https://doi.org/10.1016/j.postharvbio.2022.111981
Xu T, Wang Z, Lei T, Lv C, Wang J, Lu J (2015) New flavonoid glycosides from *Sedum aizoon* L. Fitoterapia 101:125–132. https://doi.org/10.1016/j.fitote.2014.12.014
Yıldırım MA, Goh KI, Cusick M, Barabási AL, Vidal M (2007) Drug-target network. Nat Biotechnol 25:1119–1126. https://doi.org/10.1038/nbt1338
Yin H, Xu L, Poter NA (2011) Free radical lipid peroxidation: mechanisms and analysis. Chem Rev 111(10):5944–5972. https://doi.org/10.1021/cr200084z
Zambounis A, Ganopoulos I, Valasiadis D, Karapetsi L, Madesis P (2020) RNA sequencing-based transcriptome analysis of kiwifruit infected by *Botrytis cinerea*. Physiol Mol Plant P 111:101514. https://doi.org/10.1016/j.pmpp.2020.101514
Zhao L, He F, Li B, Gu X, Zhang X, Dhanasekaran S, Zhang H (2022) Transcriptomic analysis of the mechanisms involved in enhanced antagonistic efficacy of *Meyerozyma guilliermondii* by methyl jasmonate and disease resistance of postharvest apples. LWT 160:113323. https://doi.org/10.1016/j.lwt.2022.113323
Zuo X, Li S, Hall J, Mattern MR, Tran H, Shoo J, Tan RB, Weiss SR, Butt TR (2005) Enhanced expression and purification of membrane proteins by SUMO fusion in *Escherichia coli*. J Struct Funct Genomics 6:103–111. https://doi.org/10.1007/s10969-005-2664-4